This article has been accepted for publication in a future issue of this journal, but has not been fully edited. Content may change prior to final publication. Citation information: DOI 10.1109/TNSRE.2020.2980440, IEEE Transactions on Neural Systems and Rehabilitation Engineering

Estimation of muscle co-activations in wrist rehabilitation after stroke is sensitive to motor unit distribution and action potential shapes

Božidar Potočnik, *Member, IEEE*, Matjaž Divjak, *Member, IEEE*, Filip Urh, *Student Member, IEEE*, Aljaž Frančič, *Student Member, IEEE*, Jernej Kranjec, *Member, IEEE*, Martin Šavc, *Member, IEEE* Imre Cikajlo, Zlatko Matjačić, Matjaž Zadravec, Aleš Holobar, *Member, IEEE*

***Abstract*— We evaluated different muscle excitation estimation techniques, and their sensitivity to Motor Unit (MU) distribution in muscle tissue. For this purpose, the Convolution Kernel Compensation (CKC) method was used to identify the MU spike trains from High-Density ElectroMyoGrams (HDEMG). Afterwards, Cumulative MU Spike Train (CST) was calculated by summing up the identified MU spike trains. Muscle excitation estimation from CST was compared to the recently introduced Cumulative Motor Unit Activity Index (CAI) and classically used Root-Mean-Square (RMS) amplitude envelop of EMG. To emphasize their dependence on the MU distribution further, all three muscle excitation estimates were used to calculate the agonist-antagonist co-activation index.**

We showed on synthetic HDEMG that RMS envelopes are the most sensitive to MU distribution (10 % dispersion around the real value), followed by the CST (7 % dispersion) and CAI (5 % dispersion). In experimental HDEMG from wrist extensors and flexors of post-stroke subjects, RMS envelopes yielded significantly smaller excitations of antagonistic muscles than CST and CAI. As a result, RMS-based co-activation estimates differed significantly from the ones produced by CST and CAI, illuminating the problem of large diversity of muscle excitation estimates when multiple muscles are studied in pathological conditions. Similar results were also observed in experimental HDEMG of six intact young males.

***Index Terms* — muscle co-activation, motor unit distribution, motor unit action potential, high-density surface electromyograms**

I. Introduction

Estimation of muscle excitation from surface electromyograms (EMG) is a long-standing problem that has been tackled by many different studies [7][9][12][13][16]. A surface EMG is a highly interferential signal, consisting of contributions of many Motor Units (MUs). Therefore, its exact interpretation is a difficult and not yet fully solved problem. Most of the existing studies base the muscle excitation estimation on amplitude envelopes of EMG that are easy to calculate, but contain two different classes of information. The first class comprises neural commands sent by the Central Nervous System (CNS) in the form of binary codes. Namely, by building on the all-or-nothing principle of motor neuron activation, CNS uses frequency modulation to govern the movements of skeletal muscles. In the muscles, these binary codes get amplified electrically and filtered by the Motor Unit Action Potentials (MUAPs) [3][4], which dorm the second class of information in EMG. Namely, MUAP shapes depend on many geometrical, anatomical and acquisition parameters [7]. Although beneficial when determining peripheral nervous system properties like Motor Unit Conduction Velocity [15], the MUAP shapes carry no information on neural codes and should, thus, be removed from the muscle excitation estimates. In other words, the MUAPs depend significantly on the MU distribution within the muscle tissue, and weight the neural codes with substantially different ponders in EMGs. This increases the variability of muscle excitation estimates across different muscles, subjects or contraction levels.

The estimated excitation levels are frequently normalized by the measurements at Maximum Voluntary Contraction (MVC) levels. Although aiming to standardize the relative muscle excitation levels in different subjects, this normalization may further increase the variability of excitation estimations due to the heterogeneous low- and high-threshold MU distributions in muscle tissue [2][11][18]. Moreover, amplitude envelopes have been used extensively in determination of muscle co-activation patterns and in studies of muscle synergies [17]. When comparing the excitations of different muscles, the aforementioned negative impact of MUAPs increases, due to the anatomical differences of the investigated muscles [19]. This problem increases further in different pathologies, such as stroke, where MU sizes, or their distribution within the muscle tissue, are altered.

To the best of our knowledge, these methodological limitations of muscle excitation estimation have not been fully investigated, mainly due to the lack of methodologies for efficient removal of MUAPs from EMG measurements. Namely, while the decomposition of EMG signals to contributions of different MUs removes the MUAPs [6][7][12], it also limits the number of identified MUs,

This study was supported by the Slovenian Research Agency (Projects J2-7357 and L7-9421 and Program funding P2-0041).

B. Potočnik, M. Divjak, F. Urh, A. Frančič, J. Kranjec, M. Šavc and A. Holobar are with the Faculty of Electrical Engineering and Computer Science, University of Maribor, Maribor, Slovenia (corresponding authors: bozidar.potocnik@um.si, ales.holobar@um.si).

I. Cikajlo Z. Matjačić and M. Zadravec are with the University Rehabilitation Institute, Republic of Slovenia - Soča, Ljubljana, Slovenia.

This article has been accepted for publication in a future issue of this journal, but has not been fully edited. Content may change prior to final publication. Citation information: DOI 10.1109/TNSRE.2020.2980440, IEEE Transactions on Neural Systems and Rehabilitation Engineering

opening the question of their representativeness (Fig. 1). Furthermore, full EMG decomposition is a computationally intensive procedure.

Recently, Cumulative Motor Unit Activity Index (CAI) methodology has been introduced [10], supporting the real-time MUAP compensation in EMG. In this study, we evaluated its potential to estimate the muscle co-activations in one DOF movements. First, we performed evaluation on synthetic High-Density EMG (HDEMG) signals with exactly known MU excitation patterns. Next, the CAI performance was evaluated on a group of intact and post-stroke subjects during robot-assisted wrist rehabilitation.

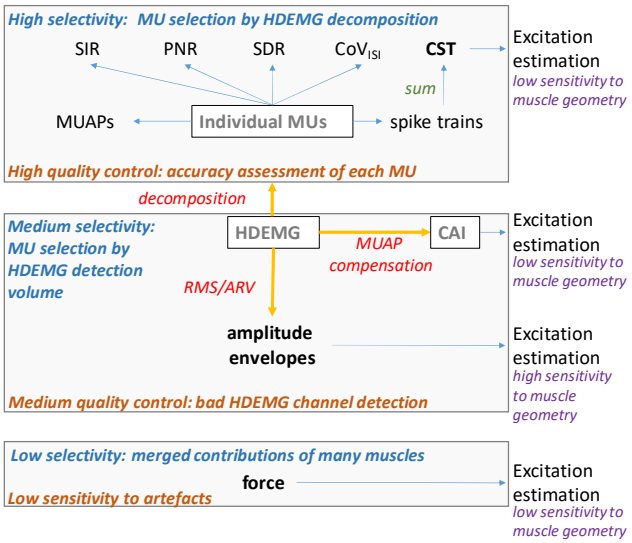

Fig. 1: Schematic comparison of different muscle excitation estimation techniques.

II. Muscle Co-Activation Estimation

A. HDEMG signals

In isometric contractions, HDEMG can be modeled by the following convolutive model [6]:

$$\boldsymbol{y}(n) = \mathbf{H}\mathbf{t}(n) + \boldsymbol{\omega}(n), \tag{1}$$

where

$$\boldsymbol{y}(n) = [y_1(n) \dots y_1(n-F-1) \dots y_M(n-F-1)]^T$$

contains the blocks of F consecutive samples of each HDEMG channel, $\boldsymbol{\omega}(n) = [\omega_1(n) \dots \omega_M(n-F-1)]^T$ is noise vector and

$$\mathbf{t}(n) = \left[t_1(n) \dots t_1(n-L-F+1) \dots t_J(n-L-F+1)\right]^T$$

contains blocks of consecutive L+F samples from all the J MU spike trains, where L stands for MUAP length in the samples. The j-th MU spike train is defined as:

$$t_j(n) = \sum_k \delta\left(n - \tau_j(k)\right), \quad j=1,\dots,J \tag{2}$$

where $\delta(.)$ is the unit-sample pulse and the k-th firing of the j-th MU appears at time $\tau_j(k)$. The mixing matrix

$$\mathbf{H} = \begin{bmatrix} \boldsymbol{H}_{11} \cdots \boldsymbol{H}_{1J} \\ \vdots \ \ddots \ \vdots \\ \boldsymbol{H}_{M1} \cdots \boldsymbol{H}_{MJ} \end{bmatrix}, \tag{3}$$

combines the blocks of MUAPs as detected by the i-th uptake electrode:

$$\mathbf{H}_{ij} = \begin{bmatrix} h_{ij}(1) & \dots & h_{ij}(L) & \dots & 0 \\ \vdots & \ddots & \ddots & \ddots & \vdots \\ 0 & \dots & h_{ij}(1) & \dots & h_{ij}(L) \end{bmatrix}. \tag{4}$$

Extension factor F [6] is usually set to values between 1 and 15, where higher values improve the conditionality of the mixing model (1) and, thus, the compensation of $\mathbf{H}$ in HDEMG decomposition and CAI (see next subsections), but also increase the computational intensity of $\mathbf{H}$ compensation. Therefore, the compromise between these two factors needs to be carefully evaluated.

B. HDEMG decomposition

The Convolution Kernel Compensation (CKC) technique cancels out the MUAPs in the model (1) and estimates the MU spike train as [6]:

$$\hat{t}_j(n) = \mathbf{c}_{t_j\boldsymbol{y}}^T \mathbf{C}_{\boldsymbol{y}}^{-1} \boldsymbol{y}(n) \approx \mathbf{c}_{t_j\mathbf{t}}^T \mathbf{C}_{\mathbf{t}}^{-1} \mathbf{t}(n) \tag{5}$$

where $\mathbf{C}_{\boldsymbol{y}} = E(\boldsymbol{y}(n)\boldsymbol{y}^T(n))$ and $\mathbf{C}_{\mathbf{t}}(n) = E(\mathbf{t}(n)\mathbf{t}^T(n))$ stand for the correlation matrix of HDEMG and MU spike trains, respectively, with $E(.)$ denoting mathematical expectation, and $\mathbf{c}_{t_j\boldsymbol{y}} = E\left(t_j(n)\boldsymbol{y}^T(n)\right)$ and $\mathbf{c}_{t_j\mathbf{t}} = E\left(t_j(n)\mathbf{t}^T(n)\right)$ are cross-correlation vectors.

The Cumulative Spike Train (CST) is then calculated by summing up the spike trains of identified MUs [13]:

$$CST(n) = \sum_j \hat{t}_j(n) \tag{6}$$

C. Cumulative Activity Index

The Activity Index (AI) in each sample n is defined as [6]:

$$\begin{aligned} AI(n) = \boldsymbol{y}(n)^T \mathbf{C}_{\boldsymbol{y}}{}^{-1} \boldsymbol{y}(n) \approx \\ \mathbf{t}(n)^T \mathbf{H}^T \mathbf{H}^{-T} \mathbf{C}_{\mathbf{t}}(n)^{-1} \mathbf{H}^{-1} \mathbf{H}\mathbf{t}(n) = \\ \mathbf{t}(n)^T \mathbf{C}_{\mathbf{t}}{}^{-1} \mathbf{t}(n) \end{aligned} \tag{7}$$

By summing up K consecutive AI values, we get the Cumulative AI (CAI), which cancels out the MUAP shapes and reveals the cumulative MU spike train [10]:

$$CAI(n,K) = \sum_{k=n-K+1}^{n} AI(k) \tag{8}$$

D. Spatially averaged RMS of HDEMG signals

RMS values of all the HDEMG channels were computed on the predefined intervals of the length of K samples. Afterwards, we computed the spatial average of RMS values over all the HDEMG channels.

Fig. 1 presents a schematic comparison of all three muscle excitation estimation techniques. HDEMG decomposition has superior quality control, but also the highest selectivity. As a result, it provides highly accurate activation estimation for the lowest number of MUs. Amplitude envelopes and CAI have medium quality control, mainly at the level of EMG signals,

This article has been accepted for publication in a future issue of this journal, but has not been fully edited. Content may change prior to final publication. Citation information: DOI 10.1109/TNSRE.2020.2980440, IEEE Transactions on Neural Systems and Rehabilitation Engineering

and exhibit medium selectivity. However, amplitude envelopes are more sensitive to muscle geometry and MUAP shapes than CAI.

III. Data acquisition and analysis

A. Synthetic HDEMG signals

We used a multilayer cylindrical volume conductor model [4] to simulate the biceps brachii muscle with 500 active MUs distributed randomly in an elliptical muscle cross-section. Average fiber density was set to 20 fibers/mm^2 [1] and fiber length was set to 130 mm. A 25 mm thick bone, 30 mm thick muscle, 4 mm thick fat and 1 mm thick skin layer were simulated [4]. The MU innervation number ranged from 24 to 2408 fibers. MUAP conduction velocity was normally distributed with the mean value of 4.0 ± 0.3 m/s.

MU recruitment thresholds and firing rates were computed by the model proposed in [5], with the parameters adapted to the biceps brachii muscle. MU recruitment thresholds were generated randomly from exponential distribution with many low-threshold MUs, and the last MU recruited at 80% of maximum excitation level [11]. MU firing rates increased linearly from 8 pulses per second (pps) at MU recruitment to 35 pps at 100% excitation. For each MU, a normally distributed InterSpike Interval (ISI) was generated with Coefficient of Variation (CoV) equal to 20 %. Ten 20 s long ramp contractions were simulated, from 0 % to 100 % and back to 0% excitation. In each simulated ramp, the MU territories were distributed randomly in the muscle, whereas the muscle excitation pattern (MU recruitment and firing patterns) were kept the same in all the simulated ramps.

Synthetic HDEMG signals were detected by an array of 9 ×10 electrodes, with a radius of 1 mm and 5 mm inter-electrode distance. HDEMG signals were computed at 4,096 samples/s and downsampled to 2,048 samples/s.

B. Experimental HDEMG signals

Six intact young males and four post-stroke subjects participated in the study, which was performed at the University Rehabilitation Institute, Republic of Slovenia - Soča. Post-stroke subjects' characteristics are listed in Table I. The experiment was conducted in accordance with the Declaration of Helsinki, and was approved by the local Ethics Committee. Each participant received a detailed explanation of the study and gave written informed consent before his participation in the study.

We fixed two arrays of 5×13 electrodes (diameter of 1 mm, interelectrode distance of 8 mm, OT Bioelettronica, Italy) to the upper third of the dominant forearm. Electrode columns were approximately perpendicular to the muscle fibers, and covered about three-quarters of the forearm circumference. The recorded HDEMG signals were amplified, band-pass filtered (3 dB, 10-900 Hz) and sampled at 2048 Hz, with 12 bits` resolution (USB EMG 2 amplifier, OT Bioelettronica, Italy).

Subject's wrist movements were opposed by a Universal Haptic Device (UHD) robot [14]. The same robot measured exerted muscle forces and wrist positions at a sampling rate of 200 Hz and 12-bits` resolution (PCI-6023E, National Instruments Inc., USA). The trigger signal recorded by both amplifiers was used to synchronize HDEMG and force signals.

All the participants performed 3 s long maximum voluntary (MVC) contractions of tested muscles. In post-stroke subjects, we measured ten repetitions of wrist flexions and extensions at ~40-60 % MVC level. In order to increase the co-activation of wrist muscles, intact persons performed ten repetitions of wrist pronation at 20 % MVC level.

TABLE I
Characteristics of post-stroke subjects

	P1	P2	P3	P4
Age	66	58	53	64
Sex	Male	Male	Male	Male
Height	175	178	173	180
Weight	98	105	70	74
Diagnosis	Stroke /hemi-plegia	Stroke /hemi-plegia	Stroke /hemi-plegia	Stroke /hemi-plegia
Affected side	right	right	right	right

C. Data analysis

HDEMG signals were extended by factor F=10, and decomposed by the CKC technique [6]. Previously introduced Pulse-to-Noise Ratio (PNR) [8] was used for quality control of identified MUs. Only MUs with PNR > 30 dB (accuracy > 90% [8]) were kept for further analysis. In each contraction their spike trains were summed up to yield CST as defined by Eq. (6) and averaged by a window of length of 0.125 s.

A similar procedure was followed for CAI calculation. First, HDEMG signals were extended by extension factor F, set to 1, 2, 5 and 10, respectively. Next, Eqs. (7) and (8) were used to calculate CAI, with parameter K set to 256 samples (0.125 s).

Spatially averaged RMS values of HDEMG signals were low-pass filtered by the window of length of 0.125 s.

In experimental conditions, calculated CST, CAI and RMS values were normalized by their maximal values, calculated from MVC recordings, yielding the muscle excitation estimate in % of maximal excitation. Afterwards, the coefficient of co-activation (CoA) was computed by dividing (in element-wise fashion) the estimated excitation of the antagonist with the estimated excitation of the agonist muscle.

In synthetic HDEMG, no further normalization was required as ramps already contained the 100 % excitation. Two different ramps were used as signals from agonist and antagonist muscles, whereat the results were averaged over all the possible ramp pairs. As exactly the same MU firing patterns were used in all the ramps, and only MU distribution within the muscle tissue was changed, the CoA should be equal to 1 in all the time instants and for all the ramp pairs.

The performance of CST, CAI and RMS techniques was measured by comparing mutually the excitation and CoA values. For HDEMG decomposition, we also calculated the Number of MUs (No. MUs), Smoothed Discharge Rate (SDR), and CoV for interspike interval (CoV_{ISI}). The Lilliefors test was used to check for normal distribution of CoA, No. MUs, SDR and CoV_{ISI} values. Normal distribution was rejected in all of them, therefore, a non-parametric Friedman test (paired comparison) and Kruskal-Wallis test

This article has been accepted for publication in a future issue of this journal, but has not been fully edited. Content may change prior to final publication. Citation information: DOI 10.1109/TNSRE.2020.2980440, IEEE Transactions on Neural Systems and Rehabilitation Engineering

(unpaired comparison) were used for further statistical analysis. All the significant effects were corrected by a Bonferroni test with significance level set to $P < 0.05$.

IV. Results

A. Synthetic HDEMG signals

On average, the CKC method identified 28 ± 4 MUs. Fig. 2 depicts representative examples of muscle excitation estimation (right panels) and CoA (left panels), estimated by CST, CAI and RMS techniques.

Statistical comparison of CoA estimations is provided in Fig. 3. CAI values for four different extension factors (F=1, F=2, F=5 and F=10) are depicted, whereas CST and RMS methods were, in all cases, estimated with the extension factor F=10 and F=1, respectively. All three techniques yielded approximately the same mean CoA value, but the RMS and CST methods exhibited significantly larger variability of CoA estimates than CAI (Fig. 3, lower panel). Noteworthy, the variability of the CST method depended significantly on the number of identified MUs, and SD of CoA estimates increased to 13 ± 4 %, 22 ± 13 % and 26 ± 15 % when only 20, 10 and 5 MUs were used for CST calculation in Eq. (6).

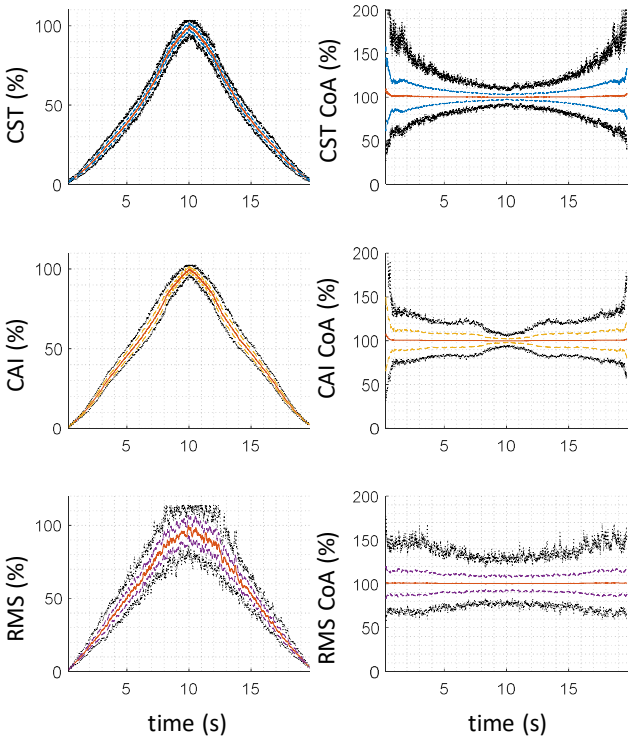

Fig. 2: Muscle excitation and CoA estimated by CST (F=10), CAI (F=5) and RMS (F=1) methods. The results are averaged over 10 synthetic HDEMG signals. Mean value is depicted in red, Standard Deviation (SD) in colored dashed lines, and minimum and maximum values in black dotted lines.

B. Experimental HDEMG signals

In intact young males, CKC identified 5.5 ± 3.3 MUs and 8.5 ± 3.3 MUs from wrist extensors and flexors, respectively. The muscle excitation values, as estimated by CST, CAI and RMS methods, are depicted in Fig. 4, along with two CoA values, namely one for the extensors vs. flexors ratio, and one for the flexors vs. extensors ratio. Due to the relatively low number of reliably identified MUs, CST-based estimates of CoA exhibited relatively large variability. This agrees with simulation studies. On the other hand, the excitation levels and CoA estimated by CAI demonstrated relatively low intra- and inter-subject variability.

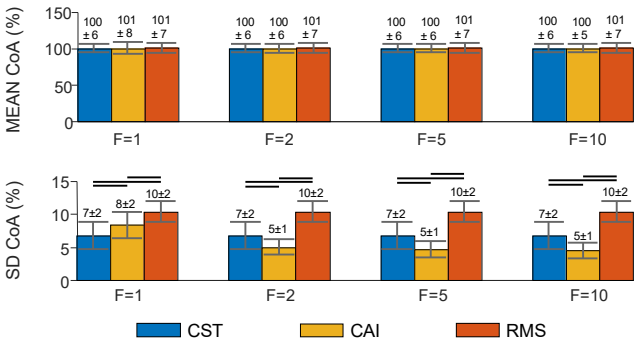

Fig. 3: Comparison of CAI-based CoA estimation (%) with CST and RMS on synthetic HDEMG signals with simulated CoA of 1 (100 %). Mean (upper panel) and SD values (lower panel), computed over time for four different extension factors F, are depicted. CST and RMS were always estimated with the extension factor F=10 and F=1, respectively. Horizontal lines denote significant differences ($p<0.05$).

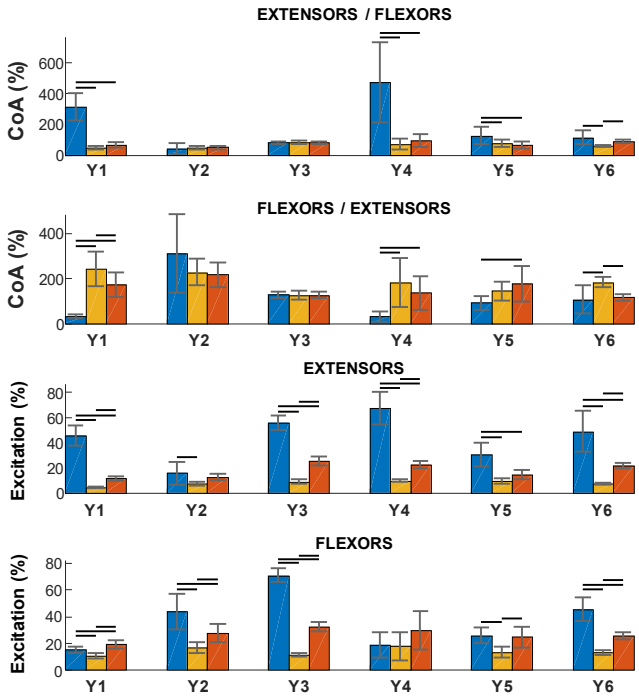

Fig. 4: Excitations of extensors and flexors and corresponding extensors vs. flexors and flexors vs. extensors CoA estimated by CST (F=10), CAI (F=10), and RMS (F=1) method from experimental HDEMG signals of six intact young males. Horizontal black lines denote significant differences (Friedman test with Bonferroni correction, $P<0.05$).

A representative example of MU identification in a post-stroke subject is presented in Fig. 5. Seven and eleven MUs were detected from wrist extensors and flexors, respectively. Unstable firing patterns are clearly visible.

This article has been accepted for publication in a future issue of this journal, but has not been fully edited. Content may change prior to final publication. Citation information: DOI 10.1109/TNSRE.2020.2980440, IEEE Transactions on Neural Systems and Rehabilitation Engineering

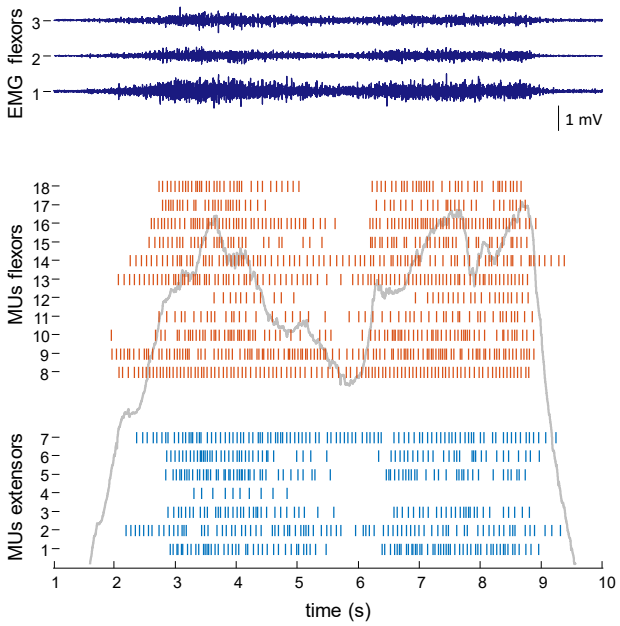

Fig. 5: MU firings identified from wrist extensors and flexors during wrist flexion task in subject P1. Each vertical bar denotes MU firing. Measured force signal is depicted by a solid gray line. The upper panel depicts three out of 64 EMG channels, recorded from wrist flexors.

Statistical results of MU identification in a post-stroke subject are presented in Fig. 6. The number of identified MUs was significantly larger in flexors during flexion than in extensors during extension. At the same time, the number of identified MUs in flexors during extension was significantly larger than the number of MUs in extensors during the flexion, indicating the larger pathological co-activation in flexors than in extensors. In accordance with these results, the SDR of extensors in extension was significantly higher than other SDRs. Furthermore, in two post-stroke subjects, (P2 and P3), SDRs of flexors in flexion and extension were not significantly different. MUs in extensors had significantly larger CoV_{ISI} than MUs in flexors.

In flexion, MUAPs had consistently larger RMS values in flexors than in extensors. On the other hand, during the extension, the MUAPs of flexors were significantly smaller than MUAPs of extensors in subject P3 only. This is at least partially in agreement with the results on MU firing patterns, where we observed larger pathological co-activation of flexors in extension than extensors in flexion.

Fig. 7 depicts the CoA values, estimated by CST, RMS and CAI from experimental HDEMG signals of post-stroke subjects. In extension, RMS yielded significantly lower CoA values than the CST and CAI techniques. In flexion, this trend was less obvious, and in subject P3, RMS yielded CoA values that are comparable to CST and CAI. In three subjects, the CST-based CoA values were significantly larger in extension than in flexion (Fig. 8). The same was true for CAI-based CoA estimates in subjects P1, P2 and P4, whereas for RMS this trend was observed in subjects P1 and in P4 only. In agreement with simulations, CST-based CoA values demonstrated the largest variance, revealing their dependence on the number of identified MUs.

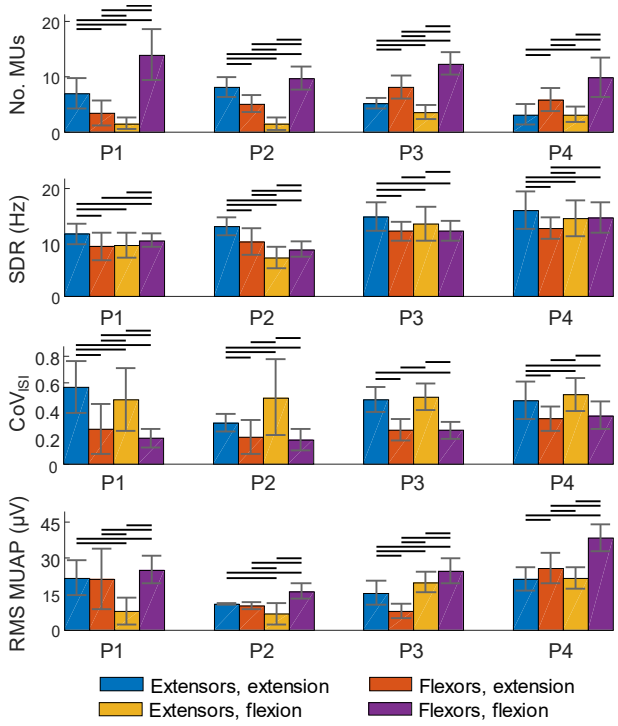

Fig. 6: No. of MUs, SDR, CoV_{ISI}, and RMS value of MUAPs identified from wrist flexors and extensors in four post-stroke subjects. Horizontal black lines denote the statistically significant differences (Kruskal-Wallis test, $P<0.05$).

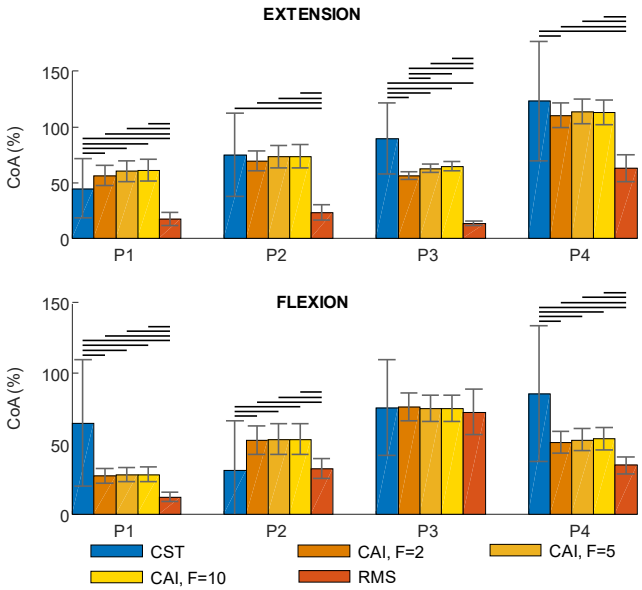

Fig. 7: CoA estimated by CST (F=10), CAI with different extension factors F and RMS (F=1) in experimental HDEMG signals from four post-stroke subjects. Horizontal black lines denote significant differences (Friedman test with Bonferroni correction, $P<0.05$). In most cases CoA values estimated by CAI with different extension factors F do not show significant differences.

Figs. 9 and 10 depict the muscle excitation levels in extension and flexion as estimated by different estimation techniques, including measured force. Interestingly, RMS yielded significantly lower excitation levels of antagonists

This article has been accepted for publication in a future issue of this journal, but has not been fully edited. Content may change prior to final publication. Citation information: DOI 10.1109/TNSRE.2020.2980440, IEEE Transactions on Neural Systems and Rehabilitation Engineering

(flexors in extension and extensors in flexion) than CST and CAI. The results on agonists were more comparable, though in most of the cases, significant differences were observed between the tested excitation estimation methods.

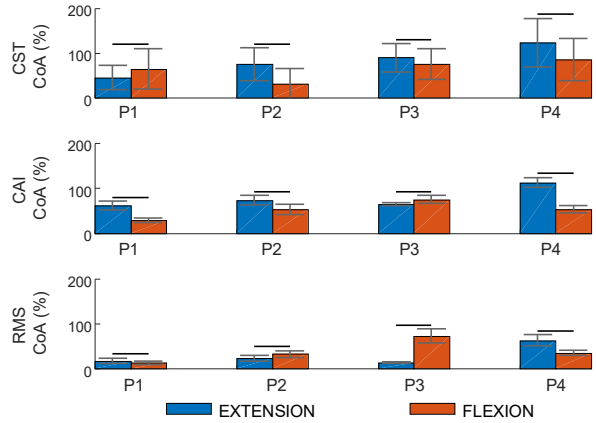

Fig. 8: CoA estimated by CST and CAI (F=10) and RMS (F=1) in experimental HDEMG signals from four post-stroke subjects. Horizontal black lines denote significant differences (Kruskal-Wallis test, P<0.05).

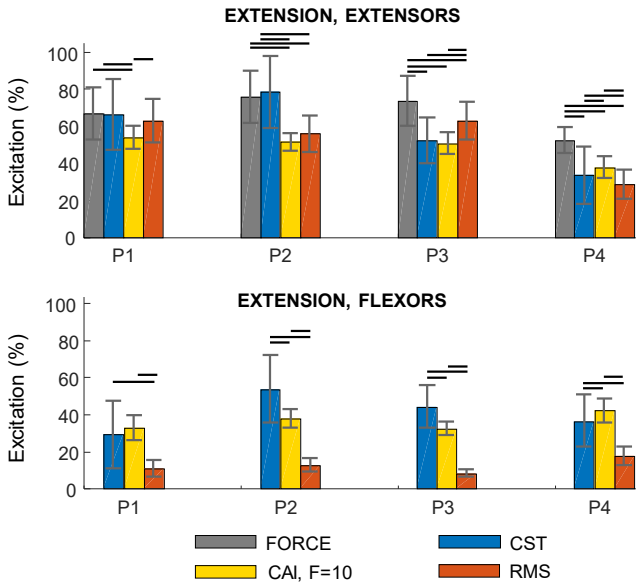

Fig. 9: Muscle excitation estimated by CST (F=10), CAI (F=10) and RMS (F=1) in post-stroke subjects during extension. Horizontal black lines denote significant differences (Friedman test with Bonferroni correction, P<0.05).

V. Discussion

We demonstrated that the amplitude envelopes of HDEMG depend significantly on the MUAP shapes and, thus, on the muscle geometry and distribution of MUs in the muscle tissue. Therefore, the impact of MUAPs needs to be removed from muscle excitation estimation. In this study, we tested two different MUAP removal techniques, namely full HDEMG decomposition to contributions of individual MUs and CAI technique proposed in [10]. Full HDEMG decomposition supports exact control of the quality, removes all impacts of noise and MUAPs from muscle estimation, but is also highly selective, as only reliably identified MUs are considered. Afterwards, identified MU spike trains are summed up into CST and low-pass filtered, to suppress the synaptic noise and emphasize the common excitation pattern of the identified motor neuron pool. As demonstrated by our simulations, when many MUs are identified, CST yields highly accurate excitation and co-activation estimates (Figs. 2 and 3), but decreases performance significantly with the decrease in the number of MUs. Moreover, as only superficial MUs get identified from HDEMG, the decomposition is not fully independent from MU distribution in the muscle tissue.

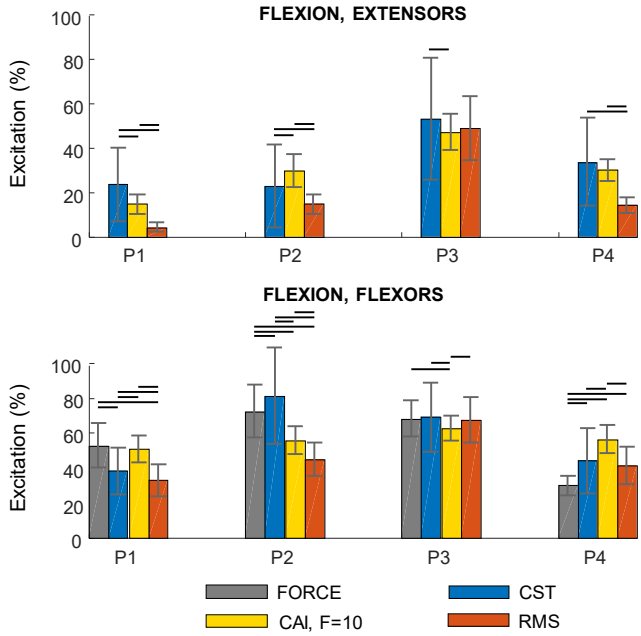

Fig. 10: Muscle excitation estimated by CST (F=10), CAI (F=10) and RMS (F=1) in post-stroke subjects during flexion. Horizontal black lines denote significant differences (Friedman test with Bonferroni correction, P<0.05).

On the other hand, CAI compensates the MUAPs and estimates CST directly, without any MU preselection. This results in a larger number of MUs being considered for muscle excitation and co-activation estimation (compared to HDEMG decomposition), but at the cost of reduced quality control. Indeed, only the quality of HDEMG channels can be currently controlled in CAI calculation. Also, CAI performance depends on the MU distribution in the muscle tissue, as HDEMG detection volume typically occupies only a portion of a muscle. However, this detection volume is usually significantly larger than the MU identification volume of HDEMG decomposition. Therefore, when extended with a sufficiently large extension factor F, CAI yields lower Standard Deviation (SD) of CoA than CST, with relatively many MUs (Figs. 2 and 3). In this study, the Standard Deviation of CAI-based CoA decreased consistently with the extension factor, though differences between F=2, 5 and 10 were not statistically significant.

RMS envelopes yielded significantly larger Standard Deviation of CoA (Figs. 2 and 3). The latter was estimated to 10 %, approximately twice the Standard Deviation of CoA values by CAI. In all the tested techniques, the Standard Deviation of CoA depended significantly on the level of muscle excitation, with the lowest Standard Deviation at the

This article has been accepted for publication in a future issue of this journal, but has not been fully edited. Content may change prior to final publication. Citation information: DOI 10.1109/TNSRE.2020.2980440, IEEE Transactions on Neural Systems and Rehabilitation Engineering

maximal excitation levels. This is a direct consequence of CoA calculation, where the excitation level of an antagonistic muscle gets divided by the excitation level of an agonistic muscle.

In post-stroke subjects, the three tested estimation techniques yielded significantly different CoA estimates, though CAI values were much closer to CST values than RMS values (Fig. 7). Detailed analysis revealed that, in most of the cases, the excitation level of antagonistic muscles was largely underestimated by RMS (Figs. 9 and 10), whereas larger agreement among the tested techniques was observed when estimating the excitation of agonists. When comparing the individual MU properties as revealed by HDEMG decomposition, we observed a relatively small number of MUs identified from extensors. When compared to flexors, extensors had also relatively small MUAPs. On the other hand, CoV_{ISI} was significantly larger in extensors than in flexors. This suggests larger difficulties in control of wrist extensors in stroke, in comparison to flexors. These findings agree with the ones reported in [16]. When estimated by HDEMG decomposition and CAI, CoA values were significantly larger during extension than flexion in three out of four subjects, confirming that flexors oppose the wrist extension significantly. Interestingly, when using the amplitude envelopes (spatially averaged RMS values in this study), the ratios between the CoA values in extension and flexion were significantly different than in the case of CST and CAI techniques (Fig. 8). In two out of the four subjects tested, co-activation during the flexion was greater than during the extension, whereas, in the remaining two subjects, co-activations in extension and flexion were much more comparable than in the case of CAI and CST estimates. The differences in CoA estimation frequently exceeded 50 %, in some cases, even 100 %. This indicates that in pathological conditions like stroke, the muscle co-activation patterns need to be interpreted with great caution.

In six intact young males, the excitation levels and CoA estimated by CAI demonstrated relatively low intra- and inter-subject variability, especially when compared to excitation levels and CoA estimated by CST and RMS techniques. Relatively large variability of values estimated by CST can be contributed to the relatively small number of accurately identified MUs.

Indeed, the Standard Deviation of CoA values estimated by HDEMG decomposition was much larger in experimental than in simulated conditions. This can be explained by at least two factors. First, the number of identified MUs was significantly larger in synthetic than in experimental conditions. Second, the number of identified MUs in the selected 0.125 s long window varied significantly in both post-stroke and intact subjects, but not in simulated conditions. Indeed, in post-stroke subjects, an abnormally large variability of MU interspike intervals and MU recruitment was observed (Figs 5 and 6). In agreement with these explanations, the variability of CAI-based estimates was significantly lower in both simulated and experimental conditions (Figs. 3, 4, 8, 9 and 10).

Both RMS-based and CAI-based estimate calculations are computationally attractive. In our tests on an Intel CORE i7 processor, they required 8.2 ± 9.0 ms and 9.8 ± 7.0 ms of a processor time per 1 second of HDEMG signals with 64 channels, respectively. In the same experimental setup, CKC-based MU identification required 19.54 ± 8.37 s per one second of HDEMG signals. Detailed analysis of the computational complexity of CST, CAI and RMS metrics is provided in [10].

In this study, the experimental signals were acquired from four post-stroke and six intact subjects only. Wide variety of specific impairments exist in each individual post-stroke subject. Our analysis was targeted at each individual tested subject (healthy and post-stroke) showing subject-specific activation and co-contraction patterns, particularly in post-stroke subjects. Thus, increasing the number of post-stroke subjects would likely increase the number of individual case studies and would not add to generalization of the results presented herein. To our belief, the tested number of post-stroke subjects has shown feasibility of the proposed approach that could be used in subject-specific robot-assisted training of isolated wrist movements where the scope and difficulty of a training task would be selected based on the outcome of EMG signal analysis as proposed in this paper.

In conclusion, we demonstrated that frequently used surface EMG envelopes are sensitive to MU distribution within the muscle tissue and can result in significant over- or underestimation of muscle co-activation. MU identification techniques remove the negative effect of MUAPs, are less sensitive to MU distribution, but their muscle excitation estimation depends severely on the number of identified MUs and stability of MU firing rates. The recently introduced CAI metric compensates MUAPs but does not aim to identify individual MUs. As such, it yields the lowest variability of muscle excitation estimation among the tested metrics, but the quality control for CAI-based estimates is yet to be developed.

REFERENCES

[1] J. B. Armstrong, P. K. Rose, S. Vanner, G. J. Bakker, and F. J. Richmond, “Compartmentalization of motor units in the cat neck muscle, biventer cervicis,” *J. Neurophysiol.*, vol. 60, no. 1, pp. 30–45, Jul. 1988.

[2] J.L. Dideriksen, A. Holobar, D. Falla: Preferential distribution of nociceptive input to motoneurons with muscle units in the cranial portion of the upper trapezius muscle, J Neurophysiol. 116(2):611-8, 2016

[3] R.M. Enoka, “Morphological features and activation patterns of motor units”. J Clin Neurophysiol., vol. 12, no. 6, pp. 538-59, 1995.

[4] D. Farina, L. Mesin, S. Martina, R. Merletti, “A surface EMG generation model with multilayer cylindrical description of the volume conductor”, IEEE Trans Biomed Eng vol. 51, pp. 415–426, 2004.

[5] A.J. Fuglevand, D.A.Winter, A.E.Patla, “Models of recruitment and rate coding organization in motor-unit pools,” J. Neurophysiol. 70, pp. 2470–88, 1993.

[6] A. Holobar and D. Zazula, "Multichannel Blind Source Separation Using Convolution Kernel Compensation", IEEE Transactions on Signal Processing, vol. 55, no. 9, pp. 4487-4496, 2007.

[7] A. Holobar and D. Farina, "Blind source identification from the multichannel surface electromyogram", Physiological Measurement, vol. 35, no. 7, pp. R143-R165, 2014.

[8] A. Holobar, M. Minetto and D. Farina, "Accurate identification of motor unit discharge patterns from high-density surface EMG and validation with a novel signal-based performance metric", Journal of Neural Engineering, vol. 11, no. 1, p. 016008, 2014.

[9] M. Jesunathadas, S.S. Aidoor, K.G. Keenan, D. Farina, R.M. Enoka, “Influence of amplitude cancellation on the accuracy of determining the onset of muscle activity from the surface electromyogram”, J Electromyogr Kinesiol., vol. 22, no. 3, pp. 494-500, 2012.

[10] J. Kranjec, A. Holobar: Improved assessment of muscle excitation from surface electromyograms in isometric muscle contractions. IEEE transactions on neural systems and rehabilitation engineering, 27(7): 1483-1491, 2019.
[11] C.G. Kukulka, H.P. Clamann, “Comparison of the recruitment and discharge properties of motor units in human brachial biceps and adductor pollicis during isometric contractions”, Brain Res., vol. 219 pp. 45–55, 1981.
[12] S. H. Nawab, S.S. Chang, C.J. De Luca, “High-yield decomposition of surface EMG signals”, Clin Neurophysiol., vol. 121, no. 10, pp. 1602-15, 2010.
[13] F. Negro and D. Farina, "Linear transmission of cortical oscillations to the neural drive to muscles is mediated by common projections to populations of motoneurons in humans", The Journal of Physiology, vol. 589, no. 3, pp. 629-637, 2011.
[14] J. Oblak, I. Cikajlo and Z. Matjacic, "Universal Haptic Drive: A Robot for Arm and Wrist Rehabilitation", IEEE Transactions on Neural Systems and Rehabilitation Engineering, vol. 18, no. 3, pp. 293-302, 2010.
[15] B. Potocnik. A. Holobar: A new optical flow model for motor unit conduction velocity estimation in multichannel surface EMG, Computers in biology and medicine, 83: 59-68, 2017
[16] K. Salonikidis, I. G. Amiridis, N. Oxyzoglou, P. Giagazoglou, G. Akrivopoulou: Wrist Flexors are Steadier than Extensors, International Journal of Sports Medicine 32(10):754-60, 2011
[17] M. Tresch, V. Cheung and A. d'Avella, "Matrix Factorization Algorithms for the Identification of Muscle Synergies: Evaluation on Simulated and Experimental Data Sets", Journal of Neurophysiology, vol. 95, no. 4, pp. 2199-2212, 2006.
[18] S.J.J. Turkawski, T.M.G.J. Van Eijden, W.A. Weijs: Force vectors of single motor units in a multipennate muscle. J Dent Res 77:1823-1831, 1998.
[19] E.J. van Zuylen, C.C. Gielen, J.J. Denier van der Gon: Coordination and inhomogeneous activation of human arm muscles during isometric torques. J Neurophysiol 60: 1523–1548, 1988.